



**HAL**  
open science

# An Inorganic Pac-Man: Synthesis, structure and electrochemical studies of a heterometallic YCo II 3 W cluster sandwiched by two germanotungstates

Masooma Ibrahim, Israël Mbomekallé, Pedro de Oliveira, Thomas Bergfeldt, Christopher Anson

## ► To cite this version:

Masooma Ibrahim, Israël Mbomekallé, Pedro de Oliveira, Thomas Bergfeldt, Christopher Anson. An Inorganic Pac-Man: Synthesis, structure and electrochemical studies of a heterometallic YCo II 3 W cluster sandwiched by two germanotungstates. *Journal of Inorganic and General Chemistry / Zeitschrift für anorganische und allgemeine Chemie*, 2022, 648 (17), 10.1002/zaac.202200112. hal-04309047

**HAL Id: hal-04309047**

**<https://hal.science/hal-04309047>**

Submitted on 27 Nov 2023

**HAL** is a multi-disciplinary open access archive for the deposit and dissemination of scientific research documents, whether they are published or not. The documents may come from teaching and research institutions in France or abroad, or from public or private research centers.

L'archive ouverte pluridisciplinaire **HAL**, est destinée au dépôt et à la diffusion de documents scientifiques de niveau recherche, publiés ou non, émanant des établissements d'enseignement et de recherche français ou étrangers, des laboratoires publics ou privés.

DOI: 10.1002/zaac.202200112

# An Inorganic Pac-Man: Synthesis, structure and electrochemical studies of a heterometallic $\{YCo^{\text{II}}_3W\}$ cluster sandwiched by two germanotungstates

Masooma Ibrahim,<sup>\*,[a]</sup> Israël M. Mbomekallé,<sup>[b]</sup> Pedro de Oliveira,<sup>[b]</sup> Thomas Bergfeldt,<sup>[c]</sup> and Christopher E. Anson<sup>[d]</sup>

Dedicated to 80th birthday of Prof. Dr. Dieter Fenske

A new heterometallic sandwich-type Keggin polyoxometalate,  $[(GeW_9O_{34})_2\{YCo(W=O)(\mu_3-O)(\mu_3-OH)(\mu_2-O)(\mu_2-OH_2)(OH_2)(C_2H_3O_2)\}]^{13-}$  has been synthesized by a simple reaction method. The isolated compound has been structurally characterized by single crystal X-ray diffraction (SC-XRD), Fourier transform infrared (FTIR) spectroscopy, elemental analysis, and thermogravimetric (TG) analysis. In addition, electrochemical

properties have been investigated in detail. The X-ray structure of this POM reveals that a unique heterometallic core  $\{YCo_3(W=O)(\mu_3-O)(\mu_3-OH)(\mu_2-O)(\mu_2-OH_2)(OH_2)(OAc)\}^{7+}$  is sandwiched between two  $[GeW_9O_{34}]^{10-}$  ligands, giving rise to the first example of a heterometallic core composed of 3d–4d–5d transition metal ions.

## Introduction

Polyoxometalates (POMs) are polynuclear metal-oxo complexes of early transition metals (e.g.  $M=V^V$ ,  $Mo^VI$ ,  $W^VI$ ,  $Ta^V$ ,  $Nb^V$ ) that are bridged by oxo ligands ( $O^{2-}$ ) to form closed 3-dimensional frameworks. They hold substantial structural and compositional versatility, allowing the tuning of their electronic structure and consequently their functionality.<sup>[1]</sup> They have demonstrated great potential in a wide range of fields, such as catalysis,<sup>[2]</sup> energy,<sup>[3,4]</sup> medicine,<sup>[5,6]</sup> imaging,<sup>[7]</sup> magnetism,<sup>[8,9]</sup> and materials science.<sup>[10]</sup> Particularly, metal-substituted POMs (MSPs) have become one of the most investigated subclasses of POMs by virtue of their structural diversity, rich redox properties and

significant applications. Lacunary POMs as multidentate O-donor ligands have a good affinity for various electrophiles, such as transition metal (TM)<sup>[11]</sup> or rare earth (RE) centers<sup>[12]</sup> to generate diverse structures with interesting properties. Among the multitude of RE-containing POMs, Y (III) embedded POMs are very limited.<sup>[13–18]</sup>

Recently, increasing interest and efforts have been devoted to the synthesis of 3d–4f heterometallic substituted POMs as one of the promising approaches to tune up the chemical and physical properties of the materials at the atomic level. However, it is still challenging to synthesize heterometallic clusters within the POM skeleton, since the oxophilic 4f cations usually possess high reactivity with highly negative polyanions, which often results in precipitation rather than crystallization. Furthermore, the difference in radius/coordination number of the 3d and the 4f centers induces competitive reactions between them which leads to the isolation of only one type of metal ion containing POMs, while the second metal type remains as a mere surface decoration or linker. So far, one-pot synthetic procedures have only succeeded in only a few examples of POM-based 3d–4f heterometallic aggregates.<sup>[19–24]</sup> The transition metal yttrium is also a rare earth element, as its chemistry and physical properties are extremely comparable to the lanthanides. Therefore, similar to 3d–4f heterometallic POMs, the exploration of 3d–Y heterometallic clusters with POM ligands also remains an ongoing challenge and the number of such materials is very small.<sup>[22,25–28]</sup>

Herein, we report the synthesis of  $Na_{10}(H_3O)_3[(GeW_9O_{34})_2\{YCo(W=O)(\mu_3-O)(\mu_3-OH)(\mu_2-O)(\mu_2-OH_2)(OH_2)(C_2H_3O_2)\}] \cdot 60H_2O$  (**Na-1**), its structural characterization in the solid state and its electrochemical behavior in aqueous solutions.

[a] M. Ibrahim

Institute of Nanotechnology (INT), Karlsruhe Institute of Technology, Hermann von-Helmholtz Platz 1, 76344 Eggenstein-Leopoldshafen, Germany

E-mail: masooma.ibrahim@kit.edu

[b] I. M. Mbomekallé, P. de Oliveira

Equipe d'Electrochimie et de Photo-electrochimie, Institut de Chimie Physique, Université Paris-Saclay, UMR 8000 CNRS, Orsay F-91405, France

[c] T. Bergfeldt

Institute for Applied Materials (IAM-AWP), Karlsruhe Institute of Technology (KIT), Postfach 3640, 76021 Karlsruhe, Germany

[d] C. E. Anson

Institute of Inorganic Chemistry, Karlsruhe Institute of Technology, Engesserstrasse 15, 76131 Karlsruhe, Germany

Supporting information for this article is available on the WWW under <https://doi.org/10.1002/zaac.202200112>

© 2022 The Authors. *Zeitschrift für anorganische und allgemeine Chemie* published by Wiley-VCH GmbH. This is an open access article under the terms of the Creative Commons Attribution Non-Commercial License, which permits use, distribution and reproduction in any medium, provided the original work is properly cited and is not used for commercial purposes.

## Results and Discussion

### Synthesis and Structure

The heterometallic cluster containing sandwich-type tungstogermanate:  $[(\text{GeW}_9\text{O}_{34})_2\{\text{YCo}(\text{W}=\text{O})(\mu_3\text{-O})(\mu_3\text{-OH})(\mu_2\text{-O})(\mu_2\text{-OH}_2)(\text{OH}_2)(\text{C}_2\text{H}_3\text{O}_2)\}]^{13-}$  (1) has been synthesized under mild bench reaction conditions by reacting  $\text{YCl}_3 \cdot 6\text{H}_2\text{O}$ ,  $\text{CoCl}_2 \cdot 6\text{H}_2\text{O}$  and the trilacunary POM ligand  $\text{Na}_{10}[\text{A-}\alpha\text{-GeW}_9\text{O}_{34}] \cdot 18\text{H}_2\text{O}$  in lithium acetate buffer solution of pH 6.6. The resultant product **Na-1** was characterized in the solid state by single crystal XRD, FTIR, TGA and elemental analysis.

The X-ray structure of 1 shows that polyanion 1 crystallized in the monoclinic crystal system with space group  $C2/m$ .

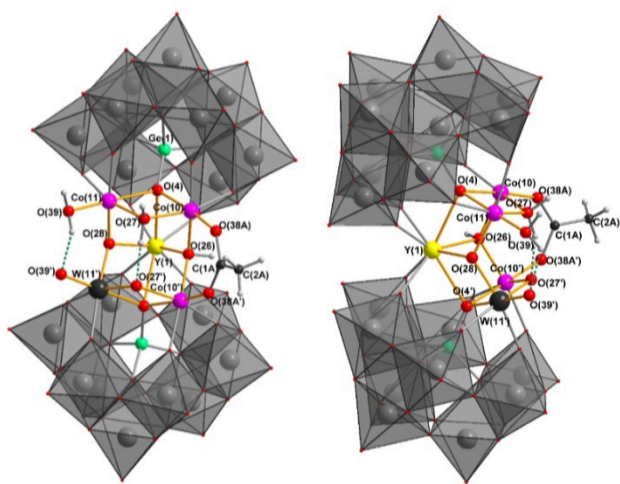


**Figure 1.** Two views of the heterometallic POM in 1, showing one of the four possible positions of the W ion within the square  $\text{Co}_3\text{W}$  face of the central  $\{\text{YCo}_3\text{W}\}$  moiety with the corresponding arrangement of ligands. The trilacunary  $(\text{GeW}_9\text{O}_{34})^{10-}$  POM metallaligands are shown in polyhedral representation, and intramolecular hydrogen bonds as green dashed lines.

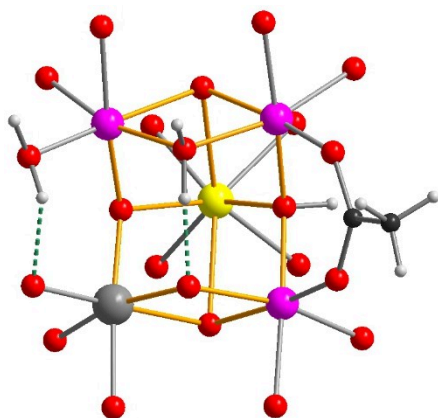


**Figure 2.** The heterometallic moiety  $\{\text{YCo}_3\text{W}\}$  in 1. Color scheme for balls: Y = yellow, Co = pink, W = dark grey, O = red, C = black, and H = light grey. Intramolecular hydrogen bonds as green dashed lines.

Polyanion 1 comprises an unprecedented, sandwich-type structure with a central heterometallic core  $\{\text{YM}_4\}$  embedded between two  $\{\text{GeW}_9\text{O}_{34}\}$  POM ligands (Figure 1). In the central pentanuclear square-pyramidal  $\{\text{YM}_4\}$  unit, one M is W(VI), equally disordered over the four M sites, the other three M are Co(II). A consequence of this metal disorder is a disorder of the ligands coordinated to the  $\text{YCo}_3\text{W}$  square-pyramid. Any oxygen atom bonded to the W atom in this moiety will be fully-deprotonated. Thus, whichever of the O(26) or the O(28) bridges between Y(1) and two Co will be  $(\mu_3\text{-OH})$ , while the other, bridging between Y(1), a Co and the W will be  $(\mu_3\text{-O})$ . Similarly, whichever of the O(27) or the O(27') bridges between two Co atoms will be  $(\mu_2\text{-OH}_2)$ , as is usual for divalent metals, while the other, bridging between Co and W, will be  $(\mu_2\text{-O})$ . For the terminal oxygen sites on these four metals, that bonded to the W will clearly be  $(\text{W}=\text{O})$ , while that on the symmetry-equivalent Co will be a water. The other pair of symmetry-equivalent metals, both being Co centres, are then bridged by a syn,syn-acetate ligand (Figure 2). The  $\text{YCo}_3\text{W}$  moiety can thus be formulated as  $\{\text{YCo}^{\text{II}}_3(\text{W}=\text{O})(\mu_3\text{-O})(\mu_3\text{-OH})(\mu_2\text{-O})(\mu_2\text{-OH}_2)(\text{OH}_2)(\mu_2\text{-}\mu^1, \mu^1\text{-OAc})\}^{7+}$ . The overall charge of the polyanion is 13+, which is balanced by 10 sodium cations and three hydronium ions  $(\text{H}_3\text{O}^+)$ . These findings are complemented by elemental analyses. Bond valence sum (BVS) gives 6.0–6.1 for the non-disordered W. Whereas, for the disordered W/Co BVS is not a reliable option to determine the valence states in a quantitative way. Apparently, the pink color of the crystals is also an indication of Co(II) and the absence of a deep blue to bronze color should mean that W mixed-valency can be excluded and so rule out any reduction to W(V). The  $\text{Y}^{\text{III}}$  ion in the heterometallic core has a square antiprismatic geometry, its coordination sites are fulfilled by six oxygen atoms from two  $[\text{GeW}_9\text{O}_{34}]^{10-}$  trilacunary ligands, one  $\mu_3\text{-OH}$  and one  $\mu_3\text{-O}$  ligands. The  $\text{Co}^{\text{II}}$  ions incorporated in the cavity of the POM ligands are hexa-coordinated, possessing an octahedral geometry. This complex is the first example of a heterometallic POM that contains a central core made up of three types of transition metals (3d–4d–5d).

### Fourier Transform Infrared Spectroscopy

The IR spectra of **Na-1** and the trilacunary ligand  $\text{Na}_{10}[\text{A-}\alpha\text{-GeW}_9\text{O}_{34}] \cdot 18\text{H}_2\text{O}$  have been recorded between 2000 and  $400\text{ cm}^{-1}$  (Figure S1, Supporting Information). They display the characteristic vibration patterns derived from the Keggin framework in the low-wavenumber region. The difference/shift in the characteristic bands of the IR spectra of the lacunary precursor and the synthesized compound indicate the formation of a new species. The characteristic vibration bands attributed to the metal-oxygen bonds observed in **Na-1** are listed in the Experimental Section.

### Thermogravimetric Analysis

The thermal stability of compound **Na-1** has been investigated in flowing  $N_2$  atmosphere with heating rate of  $10^\circ C\ min^{-1}$  in the temperature range 25–1000  $^\circ C$ . Thermogravimetric analysis (TGA) of the POM showed one successive weight loss step in the temperature range 25–925  $^\circ C$  (Figure S2, Supporting Information). The total weight loss is ca. 13%, corresponding to the removal of 41 crystal water molecules and coordinated water molecules, **hydroxo ligand** and acetate group (at higher temperatures). This result is slightly lower to the 60 water molecules determined by elemental analysis. The discrepancy may be due to different drying conditions of the bulk samples.

### Electrochemical Characterization

The electrochemistry of **Na-1** has been investigated by cyclic voltammetry (CV). Figure 3A shows the CVs of **Na-1** (black) and of the  $(GeW_9O_{34})^{10-}$  lacunary POM (red), the concentrations having been adjusted to facilitate comparison. The redox behaviours of the two compounds, although very similar, differ in some respects. The reduction process of the **Na-1** tungstic centres is slower than that of the  $\{GeW_9\}$  tungstic centres, yet the reduction peak potential value is the same for both compounds:  $-0.82\ V$  vs. SCE. During the reverse scan, the re-oxidation occurs in two distinct steps and the oxidation peak potentials are different for the two compounds (see Table 1). If the potential window is restricted between 0.6 V and  $-1.1\ V$  vs. SCE, there is no change in the surface of the working electrode

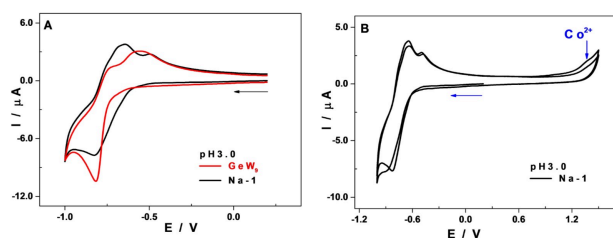


**Figure 3.** (A) CVs of **Na-1** (black) and  $GeW_9$  (red) with the potential window restricted between 0.6 V and  $-1.1\ V$ . (B) CVs of **Na-1**, two successive cycles recorded with the potential window extended up to 1.5 V. The CVs are recorded at a scan rate of  $20\ mV\cdot s^{-1}$  in 0.5 M  $Li_2SO_4 + H_2SO_4/pH\ 3.0$ . POM concentrations:  $[Na-1] = 0.33\ mM$ ,  $(GeW_9O_{34})^{10-} = 0.76\ mM$ . Working electrode: GC; counter electrode: Pt gauze; reference electrode: SCE.

**Table 1.** Reduction,  $E_c$ , and oxidation,  $E_a$ , peak potentials (mV vs SCE) measured from the CVs of **Na-1** and of  $(GeW_9O_{34})^{10-}$  recorded in the experimental conditions specified above.

	W	$E_c$	$E_{a_1}$	$E_{a_2}$	Co $E_a$
pH 3	$GeW_9$	$-0.82$	$-0.56$	$-0.73$	
	<b>Na-1</b>	$-0.82$	$-0.64$	$-0.74$	$> 1.25$
pH 5	<b>Na-1</b>	$-1.04$	$-0.80$	$-0.97$	$> 0.90$

and the electron transfer process remains controlled by diffusion (Figure S3A). When the potential window is extended to 1.5 V vs. SCE, the oxidation wave attributable to the Co(II) centres appears between 1.25 and 1.35 V vs. SCE (Figures 3B and S3B). As is often the case with the cobalt-containing POMs, the Co(II) oxidation wave is not very visible,<sup>[29]</sup> but there is a modification of the working electrode surface which results in a shift of the reduction wave towards the negative potentials during the second scan cycle (from  $-0.82\ V$  to  $-0.91\ V$  vs. SCE).

When moving to higher pH values, there is a shift of the whole CV towards the negative potential side. This results in a greater difficulty in reducing the tungstic centres, with a consequent potential shift of  $\Delta E = 220\ mV$  (Figure 4A and Table 1). On the oxidising potential side, the oxidation wave of the Co(II) centres appears at lower potentials ( $E \approx 0.9\ V$  vs. SCE), but above all it is followed by a catalytic wave attributed to the oxidation of water, a property widely observed with cobalt-containing POMs (Figure 4B).<sup>[30,31]</sup> However, the compound is only stable enough in solution for 6 hours so that its electrochemical behavior could be characterized. Since the catalytic studies require longer times (at least 24h) and the compound turned out to decay after 8h in solution, we were not able to carry them out.

### Conclusions

In summary, we have synthesized an unusual heterometallic POM  $Na_{10}(H_3O)_3[(GeW_9O_{34})_2\{YCo(W=O)(\mu_3-O)(\mu_3-OH)(\mu_2-O)(\mu_2-OH_2)(OH_2)(C_2H_3O_2)\}]\cdot 60H_2O$  (**Na-1**) under mild reaction conditions and structurally characterized it by a variety of analytical techniques such as X-ray crystallography, IR spectroscopy, elemental analysis and TGA. In addition, the electrochemical properties of **1** have also been evaluated in aqueous media. To the best of our knowledge, **Na-1** represents the first example of a 3d–4d–5d heterometallic cluster  $\{YCo^{II}_3W\}$  containing sandwich-type POM. The successful synthesis of this heterometallic POM will open the way for further exploring the heterometallic POM chemistry. The extension of this family of POMs to other 3d and 4f centers is currently in progress. We aim to explore variations to the metal ions within  $\{YCo_3W\}$  core in order to

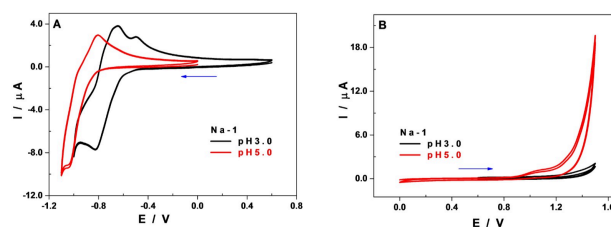


**Figure 4.** CVs of **Na-1** in 0.5 M  $Li_2SO_4 + H_2SO_4/pH\ 3.0$  (black) and in 1.0 M  $LiCH_3CO_2 + CH_3CO_2H/pH\ 5.0$  (red). (A) Potential window restricted between 0.6 V and  $-1.15\ V$ . (B) Potential window restricted between 0.0 V and 1.5 V. The CVs are recorded at a scan rate of  $20\ mV\cdot s^{-1}$ . POM concentration:  $[Na-1] = 0.33\ mM$ . Working electrode: GC; counter electrode: Pt gauze; reference electrode: SCE.

tune their electronic properties. Particularly, in case of paramagnetic 4f containing {LnCo<sub>3</sub>W}-POMs, {YCo<sub>3</sub>W}-POMs will be helpful in deleting magnetic contributions to the overall picture of paramagnetic lanthanide (Ln<sup>III</sup>) {LnCo<sub>3</sub>W} analogue through diamagnetic Y<sup>III</sup> cation.

## Experimental Section

Synthesis of Na<sub>10</sub>(H<sub>3</sub>O)<sub>3</sub>[(GeW<sub>9</sub>O<sub>34</sub>)<sub>2</sub>{YCo(W=O)(μ<sub>3</sub>-O)(μ<sub>3</sub>-OH)(μ<sub>2</sub>-O)(μ<sub>2</sub>-OH)<sub>2</sub>(OH)<sub>2</sub>(C<sub>2</sub>H<sub>3</sub>O<sub>2</sub>)}].60H<sub>2</sub>O (**Na-1**)

CoCl<sub>2</sub>·6H<sub>2</sub>O (1.07 g, 4.5 mmol) was dissolved in 100 mL of 1 M lithium acetate buffer of pH 6.6. Then, Na<sub>10</sub>[A-α-GeW<sub>9</sub>O<sub>34</sub>]·18H<sub>2</sub>O (5.33 g, 2.0 mmol) was added to this solution with stirring. Afterwards 3.0 mL of 1 M YCl<sub>3</sub>·6H<sub>2</sub>O (0.9 g, 3.0 mmol) were added to the clear pink solution. The resultant turbid solution was stirred and heated at 90 °C for one hour. Subsequently on cooling, the precipitate formed was filtered off. Slow evaporation of the solvent at room temperature for about three weeks led to the formation of pink crystals suitable for X-ray diffraction. The crystalline product was isolated using filtration and washed successively with cold water, in order to remove the traces of adsorbed acetate buffer solvent from the material before using it for bulk analysis and electrochemical studies. The bulk purity of the product was established using elemental analysis. In addition, the purity of the product was also determined by FTIR using the separated crystals of **Na-1** as reference. The perfect match of the two spectra obtained from the IR studies of separated crystals and bulk materials provide convincing evidence for purity of the bulk product (Figure S1).

Yield: 0.80 g (12 % based on W). IR ν<sub>max</sub> (cm<sup>-1</sup>; KBr pellets): 988 (w; ν<sub>as</sub>(W–O<sub>d</sub>)), 968 (w; ν<sub>as</sub>(W–O<sub>b</sub>–W)), 844 (s; ν<sub>as</sub>(Ge–O)), 849 (w; ν<sub>as</sub>(W–O<sub>c</sub>–W)), 651 and 619 (s; δ(O–Ge–O)/δ(W–O–W)), 561, 523 and 438 (m; δ(O–Ge–O)/δ(W–O–W)/δ(W–O–Ge)/δ(W–O–Y)/δ(W–O–Co)). Elemental analysis for **Na-1**, calculated (found): Na 3.54 (3.52), Ge 2.23 (2.22), Co 2.72 (2.84), Y 1.37 (1.42), W 53.72 (53.90), Y 1.37 (1.42) %.

## Crystallographic Experimental

A pink block-shaped crystal was coated in Fomblin oil and mounted on a Stoe Stadi-Vari diffractometer equipped with a MetalJet-2 liquid-Ga rotating anode source. Data were corrected for polarisation and absorption effects. The structure was solved using direct methods (intrinsic-phasing: SHELXT<sup>32</sup>) and refined by full-matrix least-squares refinement against all data (SHELXL-2018<sup>33</sup>). Ordered atoms were assigned anisotropic thermal parameters, as were the disordered metal sites Co(10)/W(10) and Co(11)/W(11).

Refinement of the metal sites Co(10) and Co(11) and their symmetry-equivalents as Co resulted in temperature factors significantly lower than for the other metal atoms in the structure. Refinement of these sites as mixed Co/W converged with occupancies close to 75 % Co and 25 % W and their temperature factors in line with those of the other metals; their Co and W occupancies were then fixed at 0.75 and 0.25, respectively, in all subsequent refinements. This results in a central square-pyramidal YM<sub>4</sub> moiety with the Y in the axial position, and three Co and one W disordered over the four basal sites. This overall formulation as a Ge<sub>2</sub>W<sub>19</sub>YCo<sub>3</sub> cluster is in excellent agreement with the metals analysis.

As a result of this disorder, no attempt was made to model the H-atoms in {YM<sub>4</sub>} moiety. Although some of the Na<sup>+</sup> counter cations and their water ligands are ordered, several are not, and again no attempt was made to model their H-atoms.

Crystallographic data for the structure in this paper have been deposited with the Cambridge Crystallographic Data Centre as supplementary publication nos. CCDC 2157252. Copies of the data can be obtained, free of charge, from <https://www.ccdc.cam.ac.uk/structures/>

## Electrochemical Characterization

Pure water was obtained with a Milli-Q Integral 5 purification set. All reagents were of high-purity grade and were used as purchased without further purification: CH<sub>3</sub>CO<sub>2</sub>H (Glacial, ProLabo Normapur), H<sub>2</sub>SO<sub>4</sub> (Sigma Aldrich), Li<sub>2</sub>SO<sub>4</sub>·H<sub>2</sub>O (Acros Organics) and LiCH<sub>3</sub>CO<sub>2</sub>·2H<sub>2</sub>O (Acros Organics). The composition of the various media was as follows: for pH 3.0, 0.5 M Li<sub>2</sub>SO<sub>4</sub> + H<sub>2</sub>SO<sub>4</sub> and for pH 5.0, 1.0 M LiCH<sub>3</sub>CO<sub>2</sub> + CH<sub>3</sub>CO<sub>2</sub>H. The stability of the compound in solution was assessed by cyclic voltammetry. ■■■■ Dear author please mention Table 2■■■■

Electrochemical data were obtained using an EG & G 273 A potentiostat driven by a PC with the M270 software. A divided cell with a standard three-electrode configuration was used for cyclic voltammetry experiments. The reference electrode was a saturated calomel electrode (SCE) and the counter electrode a platinum gauze of large surface area; both electrodes were separated from the bulk electrolyte solution via fritted compartments filled with the same electrolyte. The working electrode was a 3 mm outer diameter glassy carbon (GC) from Mersen, France. The pre-treatment of the electrode before each experiment is adapted from a method described elsewhere.<sup>[34]</sup> Prior to each experiment, solutions were thoroughly de-aerated for at least 30 min with pure argon. A positive pressure of this gas was maintained during subsequent work. All cyclic voltammograms (CVs) were recorded at a scan rate of 20 mV s<sup>-1</sup> and potentials are quoted against SCE unless otherwise stated. The polyanion concentrations were 0.16 mM for **Na-1** and adjusted for [GeW<sub>9</sub>O<sub>34</sub>]<sup>10-</sup>. All experiments were performed at room temperature, which is controlled and fixed for the laboratory at 20 °C. Results were very reproducible from one experiment to the

Table 2. Crystal Data.

Compound	Na-1
Formula	C <sub>2</sub> H <sub>137</sub> Co <sub>3</sub> Ge <sub>2</sub> Na <sub>10</sub> O <sub>139</sub> W <sub>19</sub> Y
Formula weight	6520.04
Crystal System	Monoclinic
Space Group	C2/m
a/Å	13.1860(2)
b/Å	37.8503(6)
c/Å	22.4343(3)
β/°	99.722(1)
V/Å <sup>3</sup>	11036.0(3)
Z	4
T/K	180(2)
F(000)	11844
D <sub>c</sub> /Mg m <sup>-3</sup>	3.924
μ(Ga–Kα)/mm <sup>-1</sup>	29.603
Data Measured	39068
Unique Data	12478
R <sub>int</sub>	0.0784
Data with I ≥ 2σ(I)	12142
wR <sub>2</sub> (all data)	0.1673
S (all data)	1.158
R <sub>1</sub> [I ≥ 2σ(I)]	0.0609
Parameters/Restraints	727/3
Largest diff. peak/hole/eÅ <sup>-3</sup>	+ 2.22/–3.81
CCDC number	2157252

other and slight variations observed over successive runs are rather attributed to the uncertainty associated with the detection limit of our equipment (potentiostat, hardware and software) and not to the working electrode pre-treatment nor to possible fluctuations in temperature.

## Acknowledgements

M.I. thanks Prof. Annie K. Powell for continuous support and guidance. M.I. acknowledges funding by the Helmholtz Gemeinschaft through the program Science and Technology of Nanosystems (STN) and program oriented funding phase four (PoF IV). I.M.M. and P.d.O. thank the CNRS and the Université Paris-Saclay for financial support. We also thank Olaf Fuhr for performing the single crystal X-ray crystallography (SCXRC) measurement. This work was partially carried out with the support from the Karlsruhe Nano Micro Facility (KNMF), a Helmholtz research infrastructure at the Karlsruhe Institute of Technology.COST Action MOLSPIN (CA15128). Open Access funding enabled and organized by Projekt DEAL.

## Data Availability Statement

The data that support the findings of this study are available in the supplementary material of this article.

## Conflict of Interest

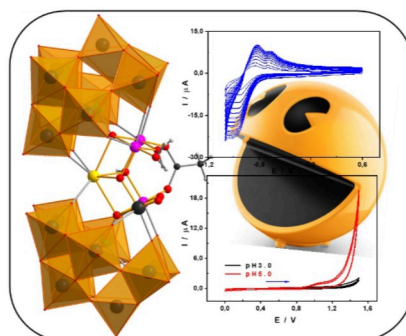
The authors declare no conflict of interest.

**Keywords:** heterometallic · polyoxometalates · yttrium · cobalt · electrochemistry

- [1] M. I. S. Verissimo, D. V. Evtuguin, M. T. S. R. Gomes, *Front. Chem.* **2022**, *10*, 1–32.
- [2] D. Gao, I. Trentin, L. Schwiedrzik, L. González, C. Streb, *Molecules* **2020**, *25*, 1–20.
- [3] M. R. Horn, A. Singh, S. Alomari, S. Goberna-Ferrón, R. Benages-Vilau, N. Chodankar, N. Motta, K. Ostrikov, J. Macleod, P. Sonar, P. Gomez-Romero, D. Dubal, *Energy Environ. Sci.* **2021**, *14*, 1652–1700.
- [4] L. Chen, W. L. Chen, X. L. Wang, Y. G. Li, Z. M. Su, E. B. Wang, *Chem. Soc. Rev.* **2019**, *48*, 260–284.
- [5] A. Bijelic, M. Aureliano, A. Rompel, *Angew. Chem. Int. Ed.* **2019**, *58*, 2980–2999; *Angew. Chem.* **2019**, *131*, 3008–3029.
- [6] A. Bijelic, M. Aureliano, A. Rompel, *Chem. Commun.* **2018**, *54*, 1153–1169.
- [7] M. Ibrahim, S. Krämer, N. Schork, G. Guthausen, *Dalton Trans.* **2019**, *48*, 15597–15604.
- [8] C. Boskovic, *Acc. Chem. Res.* **2017**, *50*, 2205–2214.
- [9] J. M. Clemente-Juan, E. Coronado, A. Gaita-Ariño, *Chem. Soc. Rev.* **2012**, *41*, 7464–7478.
- [10] A. V. Anyushin, A. Kondinski, T. N. Parac-Vogt, *Chem. Soc. Rev.* **2020**, *49*, 382–432.
- [11] S. T. Zheng, G. Y. Yang, *Chem. Soc. Rev.* **2012**, *41*, 7623–7646.
- [12] X. Ma, W. Yang, L. Chen, J. Zhao, *CrystEngComm* **2015**, *17*, 8175–8197.
- [13] M. Ibrahim, B. Bassil, U. Kortz, *Inorganics* **2015**, *3*, 267–278.
- [14] H. Lou Li, Y. J. Liu, J. L. Liu, L. J. Chen, J. W. Zhao, G. Y. Yang, *Chem. Eur. J.* **2017**, *23*, 2673–2689.
- [15] M. Ibrahim, S. S. Mal, B. S. Bassil, A. Banerjee, U. Kortz, *Inorg. Chem.* **2011**, *50*, 956–960.
- [16] J. Liu, D. Wang, X. Xu, H. Li, J. Zhao, L. Chen, *Inorg. Chem.* **2021**, *60*, 2533–2541.
- [17] K. Suzuki, M. Sugawa, Y. Kikukawa, K. Kamata, K. Yamaguchi, N. Mizuno, *Inorg. Chem.* **2012**.
- [18] M. Barsukova, M. H. Dickman, E. Visser, S. S. Mal, U. Kortz, *ZAAC* **2008**, *634*, 2423–2427.
- [19] J. Liu, Q. Han, L. Chen, J. Zhao, *CrystEngComm* **2016**, *18*, 842–862.
- [20] J. W. Zhao, Y. Z. Li, L. J. Chen, G. Y. Yang, *Chem. Commun.* **2016**, *52*, 4418–4445.
- [21] M. Ibrahim, V. Mereacre, N. Leblanc, W. Wernsdorfer, C. E. Anson, A. K. Powell, *Angew. Chem. Int. Ed.* **2015**, *54*, 15574–15578; *Angew. Chem.* **2015**, *127*, 15795–15799.
- [22] M. Ibrahim, Y. Peng, E. Moreno-Pineda, C. E. Anson, J. Schnack, A. K. Powell, *Small Structures* **2021**, *2*, 2100052.
- [23] S. Reinoso, *Dalton Trans.* **2011**, *40*, 6610–6615.
- [24] S. Reinoso, J. R. Galán-Mascarós, L. Lezama, *Inorg. Chem.* **2011**, *50*, 9587–9593.
- [25] L. Chen, J. Cao, X. Li, X. Ma, J. Luo, J. Zhao, *CrystEngComm* **2015**, *17*, 5002–5013.
- [26] G. Xue, B. Liu, H. Hu, J. Yang, J. Wang, F. Fu, *J. Mol. Struct.* **2004**, *690*, 95–103.
- [27] J. Zhao, D. Shi, L. Chen, P. Ma, J. Wang, J. Zhang, J. Niu, *Cryst. Growth Des.* **2013**, *13*, 4368–4377.
- [28] V. Das, R. Gupta, N. Iseki, M. Sadakane, A. S. Mougharbel, U. Kortz, F. Hussain, *ChemistrySelect* **2019**, *4*, 2538–2544.
- [29] C. S. Ayingone Mezui, P. De Oliveira, A. L. Teillout, J. Marrot, P. Berthet, M. Lebrini, I. M. Mbomekallé, *Inorg. Chem.* **2017**, *56*, 1999–2012.
- [30] G. Zhu, Y. V. Geletii, P. Kögerler, H. Schilder, J. Song, S. Lense, C. Zhao, K. I. Hardcastle, D. G. Musaev, C. L. Hill, *Dalton Trans.* **2012**, *41*, 2084–2090.
- [31] X. B. Han, Z. M. Zhang, T. Zhang, Y. G. Li, W. Lin, W. You, Z. M. Su, E. B. Wang, *J. Am. Chem. Soc.* **2014**, *136*, 5359–5366.
- [32] G. M. Sheldrick, *Acta Crystallogr.* **2015**, *A71*, 3–8.
- [33] G. M. Sheldrick, *Acta Crystallogr.* **2015**, *A71*, 3–8.
- [34] N. Vila, P. A. Aparicio, F. Sécheresse, J. M. Poblet, X. López, *Inorg. Chem.* **2012**, *51*, 6129–6138.

Manuscript received: March 19, 2022

Revised manuscript received: July 11, 2022



M. Ibrahim\*, I. M. Mbomekallé, P. de Oliveira, T. Bergfeldt, C. E. Anson

1 – 6

**An Inorganic Pac-Man: Synthesis, structure and electrochemical studies of a heterometallic {YCo<sup>II</sup><sub>3</sub>W} cluster sandwiched by two germanotungstates**



 ## SPACE RESERVED FOR IMAGE AND LINK

Share your work on social media! ZAAC has added Twitter as a means to promote your article. Twitter is an online microblogging service that enables its users to send and read short messages and media, known as tweets. Please check the pre-written tweet in the galley proofs for accuracy. If you, your team, or institution have a Twitter account, please include its handle @username. Please use hashtags only for the most important keywords, such as #catalysis, #nanoparticles, or #proteindesign. The ToC picture and a link to your article will be added automatically, so the **tweet text must not exceed 250 characters**. This tweet will be posted on the journal's Twitter account (follow us @ZAAC) upon publication of your article in its final (possibly unpaginated) form. We recommend you to re-tweet it to alert more researchers about your publication, or to point it out to your institution's social media team.

## ORCID (Open Researcher and Contributor ID)

Please check that the ORCID identifiers listed below are correct. We encourage all authors to provide an ORCID identifier for each coauthor. ORCID is a registry that provides researchers with a unique digital identifier. Some funding agencies recommend or even require the inclusion of ORCID IDs in all published articles, and authors should consult their funding agency guidelines for details. Registration is easy and free; for further information, see <http://orcid.org/>.

Israël M. Mbomekallé <http://orcid.org/0000-0003-3440-8066>

Pedro de Oliveira <http://orcid.org/0000-0002-4823-4143>

Thomas Bergfeldt <http://orcid.org/0000-0003-4595-7968>

Christopher E. Anson <http://orcid.org/0000-0001-7992-7797>

Masooma Ibrahim <http://orcid.org/0000-0002-8520-8585>